Interpretation of the Effect of Compaction on the Mechanical Behavior of Embankment Materials Based on the Soil Skeleton Structure Concept

Interprétation de l'effet de compactage sur le comportement mécanique des matériaux de remblai basée sur le concept de structure des sols

Sakai T., Nakano M.
International Member, Nagoya University,Japan

ABSTRACT: In this research, triaxial compression tests were carried out on 5 materials having different grain size distributions and compaction properties to determine the mechanical properties of compacted soil. In addition, the triaxial test results were reproduced using the SYS Cam-clay model to interpret the mechanical behavior of the compacted soil and the effect of compaction on soil based on the soil skeleton structure concept. Also, seismic response analysis of embankments constructed using these soils was carried out using GEOASIA to determine the relationship between the compaction properties and the seismic stability of embankments. The following were the main conclusions. 1) The maximum deviator stress increased with the increase in degree of compaction Dc, but the trends in the increase differed depending on the material. 2) The mechanical behavior of the compacted soil could be reproduced using the SYS Cam-clay model using one set of material constants for each material. 3) It was found that when the Dc is increased, the seismic stability is increased and that as the maximum dry density increased, the seismic stability increased.

RÉSUMÉ: Dans cette étude, nous étudions les caractéristiques mécaniques de sols compactés en mettant en œuvre des essais de compression triaxiale sur 5 échantillons ayant des caractéristiques de granulométrie et de compactage différentes. En outre, nous reproduisons les résultats des essais triaxiaux grâce au modèle SYS Cam-clay d'équation constitutive d'élastoplasticité. Nous avons également effectué l'analyse de la réponse sismique de la déformation des remblais ainsi créés en utilisant le programme d'analyse dynamique de déformation finie eau-sol GEOASIA pour comprendre la relation entre les caractéristiques du compactage et les performances sismiques du remblai. Les principales conclusions sont indiquées ci-dessous. 1) Avec l'augmentation du degré de compactage, la la contrainte axiale maximale est augmentée, mais cette augmentation dépend de la nature de l'échantillon. 2) Il a été possible de reproduire le comportement mécanique des sols compactés à l'aide du modèle SYS Cam-clay. 3) Quand le degré de compactage augmente, il a été constaté que plus la densité sèche maximale de l'échantillon est grande plus importante est sa résistance aux tremblements de terre.

KEYWORDS: compaction, embankment, triaxial compression test.

1 INTRODUCTION

The stability of the embankment is progressing since fundamental principle of soil compaction proposed by Proctor (Proctor, 1933), and many researcher and engineer have studied and improved quality control standard by compaction . After Han-Shin Awaji Earthquake disaster, road earthwork guideline for construction of embankment was revised to evaluate the seismic resistance of embankments, and design principles are changing from being specification based to being performance based. However, locally occurring materials are still used as embankment materials, and quality control of embankments is carried out using the Dc, so doubts remain regarding whether good quality embankments are being produced. In addition, because prediction of the deformation behavior of embankments due to earthquakes is extremely important, a theory for reproducing the mechanical behavior of compacted materials to enable prediction of the deformation behavior of embankments in an earthquake is necessary.

In this study, 5 types of soil material with different grain size distributions and compaction properties were selected, and the compacted soil specimens were subjected to $\overline{CU}$ triaxial tests, with the objective of obtaining basic data to reproduce the mechanical behavior of various materials after compaction. The shear behavior after compaction was compared and examined in accordance with the differences in the materials. In addition, the effect of compaction on the mechanical behavior of embankment materials was interpreted based on the soil skeleton structure concept by reproducing the mechanical behavior using the elasto-plastic super/subloading yield surfaces Cam-clay model (hereafter referred to as the SYS Cam-clay model) (Asaoka et al. 2002). Also, seismic stability analysis of embankments were carried out using the soil-water coupled finite deformation analysis program GEOASIA (Noda et al. 2008), which incorporates the SYS Cam-clay model, to determine the relationship between the compaction properties and the seismic stability of embankments.

2 PHYSICAL AND COMPACTION PROPERTIES OF EMBANKMENT MATERIALS

Five types of materials were examined in this study and are referred to as materials A, B, C, D, and E (Nakano et al. 2010, Yokohama et al. 2010). Fig. 1 shows the grain size distributions of the 5 materials. Fig. 2 shows the results of compaction tests on the 5 materials. The compaction tests were carried out by the A-b method for materials B and D, by the A-a method for materials A and C, and by the A-c method for material E. It can be seen that as the amount of coarse-grained fraction of the material increased, the maximum dry density increased and the optimum water content decreased.

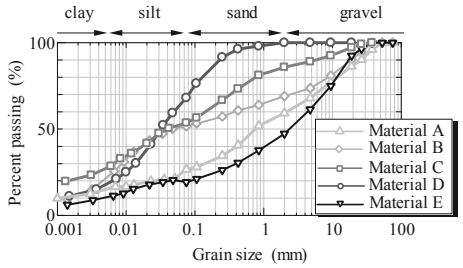

Figure 1. Grain size distribution

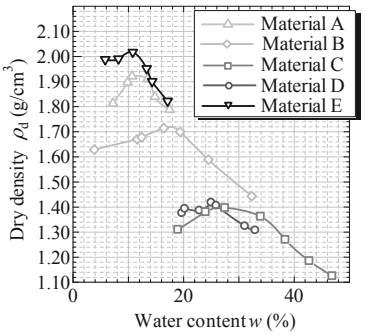

Figure 2. Compaction test results

3 EFFECT OF COMPACTION ON THE MECHANICAL PROPERTIES OF EMBANKMENT MATERIALS

For 5 types of materials, $\overline{CU}$ triaxial compression tests were carried out under Dc and confining pressure shown in Table 1. The materials D and E are omitted. When preparing the test specimens, the Dc was adjusted by changing the compaction energy. After setting the specimen in the triaxial compression apparatus, the specimen was saturated with de-aired water using the double-suction method or the back pressure method. Then isotropic consolidation process was carried out, and when it was confirmed that the consolidation completed, the undrained shearing was carried out under constant axial strain rate.

Table 1 Test conditions

	Material A	Material B	Material C
Confining pressure (kPa)	100, 300	50, 100, 150, 300	100, 300
Dc (%)	85, 90, 95, 100	85, 90, 95, 100	90, 95, 100

Fig. 3 shows that the deviator stress q – shear strain ε_s relationship and q - mean effective stress p' relationship of the $\overline{CU}$ triaxial tests when the confining isotropic consolidation pressure was 100 kPa for materials A through C. The materials D and E are omitted. In this section, the increase in q during shearing and maximum of q as a result of compaction is referred to as 'compaction effect'. For material A at the 85 and 90% of Dc, an increase in q associated with a reduction in p' was seen at the initial shear (shear strain ε_s = 0–2%). Thereafter, it exhibited the mechanical behavior of normally consolidated soil with both p' and q in a critical state. At the 95% of Dc, there was almost no reduction in p' observed, and thereafter, both p' and q exhibited a critical state. At the 100% of Dc, an increase in q associated with the increase in p' was seen, and the maximum of q increased greatly. It can be seen that if the Dc of material A is not large, a compaction effect is not seen. With material B, an increase in q associated with the increase in p' was seen at all Dc. Also, q increased continuously with the ε_s, and the behavior resembles that of pure sand specimen. However, as for material A, if the Dc of material B is not large, a compaction effect is not seen. With material C at the 90 and 95% of Dc, softening behavior was seen associated with plastic compression as a reduction in q associated with a reduction in p'. This is behavior seen in soft natural deposited clay. On the other hand, at the 100% of Dc, the shear behavior changed, with q increasing in association with an increase in p', and the compaction effect was exhibited. However, the compaction effect was small compared with materials A and B.

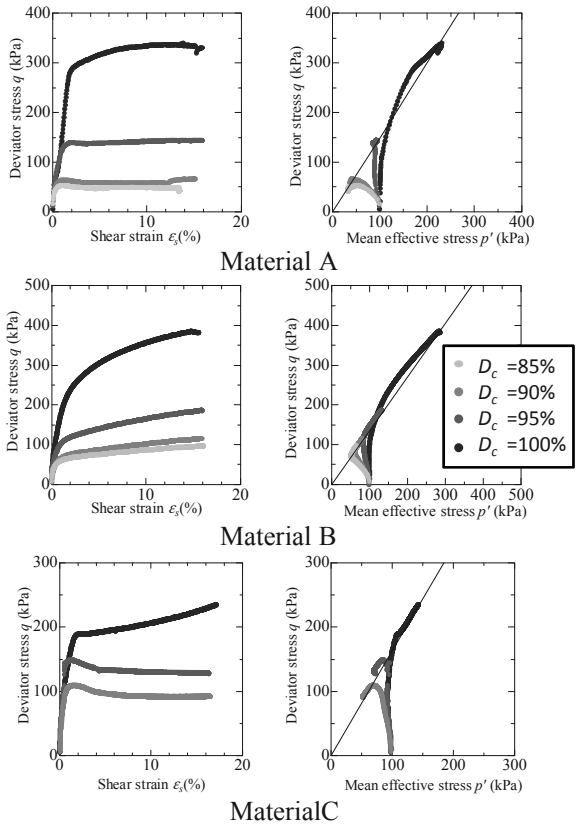

Fig. 3 Undrained triaxial test results

4 INTERPRETATION OF COMPACTION EFFECT BASED ON SOIL SKELETON STRUCTURE CONCEPT

The SYS Cam-clay model is an elasto-plastic constitutive model that expresses soil skeleton structure as 3 properties, structure, overconsolidation, and anisotropy, and describes the evolution of the soil skeleton structure associated with development of plastic deformation. The major characteristic of the SYS Cam-clay model is that it can explain the mechanical behavior of typical clays and sands, as well as intermediate soils, based on the rate of change of the evolution of the soil skeleton structure. In this study, the undrained shear behavior after compaction for 5 materials is simulated by the SYS Cam-clay model, and each compaction effect of each specimens can be interpreted based on soil skeleton structure.

Figs. 4 through 6 show the results of reproducing the mechanical behaviors of materials A through E using the SYS Cam-clay model. The top 2 graphs are the stress-strain relationship and the effective stress path, as in Fig. 3. The bottom left graph shows the decay of structure associated with shear deformation, and the bottom right graph shows how loss of overconsolidation associated with shear deformation occurred; R* indicates the degree of structure, and the closer R* is to 1, the lower the structure is, while R indicates reciprocal of OCR.

The material constants and the initial conditions of the materials are shown in Tables 3 and 4, respectively. The calculation results were able to reproduce the test results. In the case of materials for which a large maximum dry density was

obtained in the compaction test, such as material A, the decay of structure and loss of overconsolidation are fast. On the other hand, in the case of materials for which a small maximum dry density was obtained in the compaction test, such as material C, there was little decay of structure, and loss of overconsolidation was moderate. Finally, for material B, the results indicated that the decay of structure was fast and that the loss of overconsolidation was slow. As the maximum dry density increased, decay of structure occurred faster. However, there was no correlation between the rate of loss of overconsolidation and the maximum dry density. Also, focusing on the initial values, for all materials, it can be seen that as the Dc increased, the structure decayed, and overconsolidation accumulated. Also, it can be seen that for material such as C with small maximum dry densities, structure and overconsolidation tend to remain even though they are compacted. It can be inferred that this is because there is little decay of structure due to shearing. Also, focusing on materials A and B at Dc of 95–100%, overconsolidation increases suddenly as a result of compaction. At this time, the q also increases greatly. It can be seen that the increase in q of compacted soil can be determined by the ease of accumulation of overconsolidation.

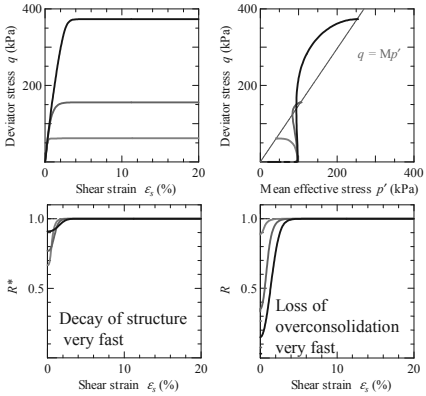

Figure 4. Material A reproduction results

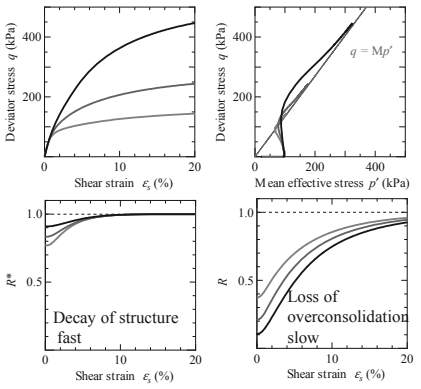

Figure 5. Material B reproduction results

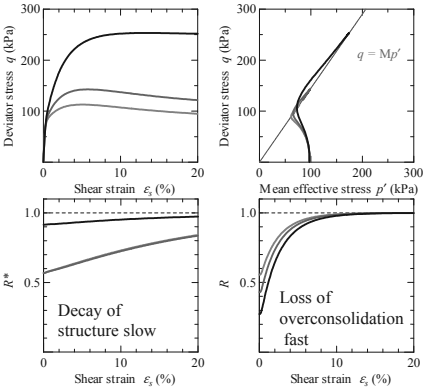

Figure 6. Material B reproduction results

Table 2 Material constants

Material		A	B	C
Elasto-plastic parameters				
Compression index		0.07	0.11	0.13
Swelling index		0.01	0.02	0.01
Limit state index		1.48	1.35	1.45
NCL intercept (98.1 kPa)		1.50	1.71	2.07
Poisson's ratio		0.30	0.30	0.30
Normal consolidation index		5.00	0.50	1.30
Evolution rule parameters				
Structure decay index	a	10.0	2.00	0.80
	b	1.00	1.00	1.00
	c	1.00	1.00	1.00
	c_s	1.00	1.00	0.40
Rotational hardening index		0.00	0.10	0.00
Rotational hardening limit constant		0.10	0.40	1.00

Table 3 Initial values

Material	Dc	Specific volume	Extent of structure	Overconsolidation
A	90	1.55	1.50	3.77
	95	1.47	1.30	13.2
	100	1.40	1.10	32.0
B	90	1.72	1.30	8.10
	95	1.64	1.20	19.1
	100	1.56	1.10	42.5
C	90	2.17	2.20	5.1
	95	2.08	1.90	9.8
	100	1.98	1.40	16.2

5 SEISMIC RESPONSE ANALYSIS OF EMBANKMENTS

Fig. 7 shows a complete cross-section of the embankment and ground used in the analysis. The ground was assumed to be hard ground with poor permeability. Also, it was made sufficiently wide to take into consideration the effects of the side surface boundaries. The height of the embankment was 6 m, with slopes of 1:1.8. Also, the width of the crown was 14 m, assuming an expressway with one lane on each side. The hydraulic boundary conditions were as shown in Fig. 7; the edges on the left, right and bottom were impermeable boundaries, and the top edge was a permeable boundary (atmosphere). Also, the water level was always constant at the ground surface. In other words, the ground and embankment were always saturated. The movement boundary conditions before the earthquake were as follows: all the nodes on the left and right edges were fixed horizontally, and all the nodes on the bottom surface were fixed horizontally and vertically. During and after the earthquake, periodic boundaries were assumed, and both edges were provided with constant displacement boundaries. In addition, in order to prevent all reflections of the seismic waves, a viscous boundary (Joyner et al. 1975) was provided in the horizontal direction on the bottom edge during the earthquake. The seismic motion is measured ground surface wave at Kobe Marine Observatory in the Southern Hyogo prefecture earthquake in 1995. The input seismic motion was assumed to be a level 2 inland earthquake. In this section, the materials analyzed were materials A and C.

Figs. 8 and 9 show the shear strain distribution immediately before and after the earthquake for materials A and C, respectively. Also, the values shown in the figures indicate the amount of settlement in the center of the crown after the earthquake. For all the materials, as the Dc is increased, the strain due to the earthquake becomes smaller, and the amount of settlement is reduced to about one-third. It can be seen that increasing the Dc is extremely effective for improving the seismic stability of embankments. For material A at all Dc, the strain due to the earthquake did not extend, and stable behavior

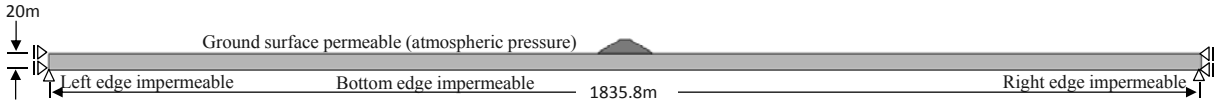

Figure 7. Analysis cross-section

was exhibited during and after the earthquake. For material C at the 90% of Dc, a slip plane occurred from the top of the slope of the embankment due to the earthquake, resulting in collapse. However, it can be seen that as the Dc increased, the shear strain due to the earthquake reduced, and the seismic stability increased. From the above, it can be seen that greater seismic stability can be obtained from embankments constructed with materials with fast decay of structure and loss of overconsolidation (material A) than from embankments constructed from materials with little decay of structure, and loss of overconsolidation (material C).

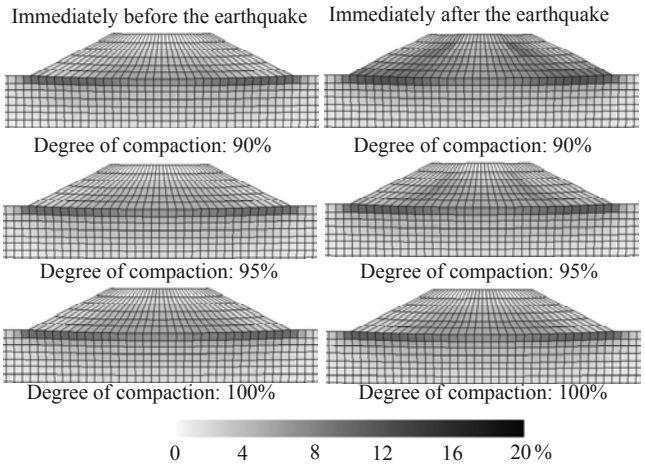

Figure 8. Shear strain distribution (material A)

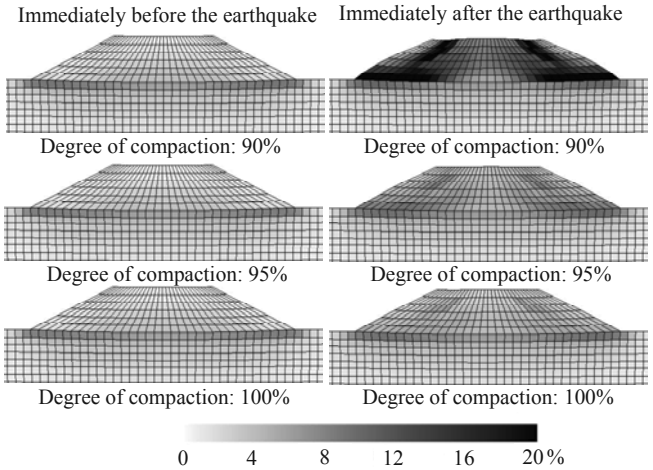

Figure 9. Shear strain distribution (material C)

6 CONCLUSIONS

In this research, various laboratory tests were carried out on 5 types of embankment material, and their mechanical behaviors were reproduced using the SYS Cam-clay model. Also, seismic response analysis was carried out for embankments constructed with 2 types of material with 3 Dc. The following are the conclusions obtained from this research.

1) For all materials, an increase in q associated with an increase in p' during shearing was seen as a result of compaction, and the maximum of q increased. However, the trend in the increase was different for each material; for some materials, the maximum of q did not increase with compaction, and for some materials, the maximum of q suddenly increased from a certain Dc.

2) The mechanical behavior of each material was reproduced with the SYS Cam-clay model using one set of material constants for each material and representing the differences in Dc by different initial conditions of structure and overconsolidation. It was possible to interpret the increase in Dc as decay of structure and accumulation of overconsolidation. When the q increased beyond CSL, it was found that the overconsolidation tended to increase. Also, it was found that a large maximum dry density, such as material A, exhibits that the decay of structure and loss of overconsolidation are fast, while a small maximum dry density, such as material C, there was little decay of structure, and loss of overconsolidation was moderate.

3) From seismic response analysis using GEOASIA, it was found that the seismic stability of embankments was increased by increasing the Dc. Materials with fast decay of structure and loss of overconsolidation, such as material A, produce embankments with high seismic stability, so they are good embankment materials.

7 ACKNOWLEDGEMENTS

Data for this report were provided by Atsuko Sato of the Civil Engineering Research Institute for Cold Region and Professor Seiichi Miura of Hokkaido University with the assistance of the 2009 Ministry of Land, Infrastructure, Transport and Tourism Construction Technology Research and Development Subsidy Program, for which we wish to express our thanks.

8 REFERENCES

Asaoka A., Noda T., Yamada E., Kaneda K. and Nakano M. 2002. An elasto-plastic description of two distinct volume change mechanisms of soils. Soils and Foundations Vol. 42, No. 6, pp.47–57.

Noda T., Asaoka A. and Nakano M. 2008. Soil-water coupled finite deformation analysis based on a rate-type equation of motion incorporating the SYS Cam-slay model. Soils and Foundations Vol. 48, No. 6, pp. 771–790.

Nakano et al. 2010. Comparison of the mechanical behavior of 2 types of soil with different compaction properties. 45th Conference on Research and Development in Geotechnical Engineering No. 133, pp. 265–266.

Yokohama et al. 2010. Effect of compaction conditions on the shear properties of sandy silt used as a material for constructing levees. Abstracts of Japan Society of Civil Engineers 65th Annual Technical Conference III-142, pp. 283–284.

Joyner W.B., Albert T. and Chen F. 1975. Calculation of nonlinear ground response in earthquakes. Bulletin of the Seismological Society of America Vol. 65, No. 5, pp. 1315–1336.

MLIT Public Works Research Institute Earthquake Disaster Prevention Research Center Vibration Research Department 2001.: Experimental survey of seismic design methods for buried structures taking large scale earthquakes into consideration, Summary Report on the Results of Experimental Survey Research by the Vibration Research Department. Vibration Research Department Document No. 22, pp. 19–20, 2001.3.